A quantitative study of valence electron transfer in the skutterudite compound $CoP_3$ by combining x-ray induced Auger and photoelectron spectroscopy



2007 J. Phys.: Condens. Matter 19 246216

(http://iopscience.iop.org/0953-8984/19/24/246216)

IOP PUBLISHING JOURNAL OF PHYSICS: CONDENSED MATTER

J. Phys.: Condens. Matter **19** (2007) 246216 (13pp) doi:10.1088/0953-8984/19/24/246216

# A quantitative study of valence electron transfer in the skutterudite compound $CoP_3$ by combining x-ray induced Auger and photoelectron spectroscopy

**S Diplas[1,2,4], Ø Prytz[1], O B Karlsen[2], J F Watts[3] and J Taftø[2]**

[1] Centre for Materials Science and Nanotechnology, University of Oslo, PO Box 1126, Blindern, NO-0318 Oslo, Norway
[2] Department of Physics, University of Oslo, PO Box 1048, Blindern, NO-0316 Oslo, Norway
[3] The Surface Analysis Laboratory, School of Engineering, University of Surrey, Guildford, Surrey GU2 7XH, UK

E-mail: spyros.diplas@fys.uio.no

Received 15 March 2007, in final form 4 May 2007
Published 24 May 2007
Online at stacks.iop.org/JPhysCM/19/246216

**Abstract**

We use the sum of the ionization and Auger energy, the so-called Auger parameter, measured from the x-ray photoelectron spectrum, to study the valence electron distribution in the skutterudite $CoP_3$. The electron transfer between Co and P was estimated using models relating changes in Auger parameter values to charge transfer. It was found that each P atom gains 0.24 $e^-$, and considering the unit formula $CoP_3$ this is equivalent to a donation of 0.72 $e^-$ per Co atom. This is in agreement with a recent electron energy-loss spectroscopy study, which indicates a charge transfer of 0.77 $e^-$/atom from Co to P.

## 1. Introduction

Compounds with the skutterudite-type structure have attracted much attention over the last decade, owing to their possible use as thermoelectric materials. These compounds have the general formula $TX_3$, with TM being a transition metal (typically Co, Rh, Ir) and X one of the pnicogens P, As or Sb. The skutterudites belong to the cubic space group $Im\bar{3}$ (Kjekshus and Pedersen 1961, Kjekshus and Rakke 1974); the metal atoms are octahedrally coordinated by the pnicogen atoms, while the pnicogens have two metal and two pnicogen nearest neighbours in a tetrahedral environment.

In an effort to understand the electronic properties and atomic bonding in binary skutterudites, several band structure calculations have been performed (Llunell *et al* 1996, Singh and Pickett 1994, Fornari and Singh 1999, Løvvik and Prytz 2004). X-ray photoelectron

[4] Author to whom any correspondence should be addressed.

spectroscopy (XPS) studies of transition metal monophosphides, $LaFe_4Sb_{12}$, $CeFe_4Sb_{12}$, $CoAs_3$, $CoSb_3$ and $RhSb_3$ (Anno *et al* 2000, Lefebvre-Devos *et al* 2001, Nemoshalenko *et al* 1983, Grosvenor *et al* 2005, 2006) employed photoelectron peak shifts and shapes, energy loss features and valence band spectra to study charge transfer and bonding phenomena. Small chemical shifts in the core binding energies of both the transition metals and pnicogens were observed for the antimonides and arsenides, indicating limited charge transfer between the constituent elements. This is consistent with the small difference in the electronegativity of these elements. A predominantly covalent bonding scheme is therefore assumed, in which the transition metal is bonded to its octahedrally coordinated pnicogens through $d^2sp^3$ hybrid orbitals, while the bonds between the pnicogens have $sp^3$ hybrid character (Uher 2001, Dudkin 1958, Kjekshus and Pedersen 1961). This bonding scheme is in qualitative agreement with band structure calculations (Koga *et al* 2005, Fornari and Singh 1999), while somewhat larger shifts for the phosphides indicate bonding of more ionic nature (Grosvenor *et al* 2006).

Recently, studies using electron energy-loss spectroscopy (EELS) indicated an emptying of the Co 3d states in $CoP_3$, $CoAs_3$ and $CoSb_3$ relative to that of the pure metal (Prytz *et al* 2007). The effect was largest for $CoP_3$, showing a reduction of approximately 0.77 $e^-$/atom, while smaller changes were observed for $CoAs_3$ and $CoSb_3$ ($\sim$0.4 $e^-$/atom). However, EELS probes a dipole-selected local density of empty states, and is therefore sensitive to both charge transfer away from the Co atoms, and hybridization effects causing a change in the degree of d-character of the valence electrons (Keast *et al* 2001). In an effort to deconvolute these effects, we compare these EELS results with results from XPS and x-ray induced Auger electron spectroscopy (XAES) which probe occupied energy states. XPS and XAES are based on the excitation of core levels, and although core electrons are not directly involved in bonding they respond to changes in the atomic environment (and to charge transfer/redistribution phenomena (a)) via energy shifts of their spectral peaks. We characterize the $CoP_3$ compound produced in a Sn flux with SEM and XRD, and we supplement XPS with XAES to probe the bonding in the $CoP_3$ crystals. In addition to the common practice of using core-level energy shifts, we monitor changes in the P 2p–Co 2p energy separation and employ the Auger parameter in the Thomas and Weightman model (1986) in order to probe atomic bonding and charge transfer phenomena. The results are discussed and compared to the literature data of pure Co, P (white), Co–P compounds and other transition metal phosphides.

## 2. Methods and materials

### *2.1. Synthesis and characterization*

Single crystals of $CoP_3$ were grown using a Sn-flux technique (Watcharapasorn *et al* 1999). Cobalt filings (Goodfellow 99.9%), pieces of red phosphorus (Koch-Light 99.999%), and tin granules (Fluka 99.999%) were loaded into a silica glass ampoule in the atomic ratio Co:P:Sn = 1:3:25, and the ampoule was evacuated and sealed. The ampoule was kept at 780 °C for one week before being slowly cooled to room temperature.

The resulting ingot was cut into two vertical sections. Light microscopy and scanning electron microscopy (SEM) combined with energy-dispersive x-ray analysis (EDX), showed that the ingot contained single crystals of $CoP_3$ dispersed in a Sn matrix (see figure 1(a)). No other phases were detected. SEM showed that the crystals (up to 300 $\mu$m in diameter) all had a composition consistent with $CoP_3$ (see figure 1(b)). Part of the unused ingot was immersed in dilute HCl (water:HCl = 1:1), which dissolved the Sn matrix, leaving the $CoP_3$ crystals un-attacked (see figure 1(b)). X-ray diffraction (XRD) was performed with a Siemens D-5000 diffractometer in Bragg–Brentano geometry using Cu K$\alpha_1$ radiation. The XRD data were

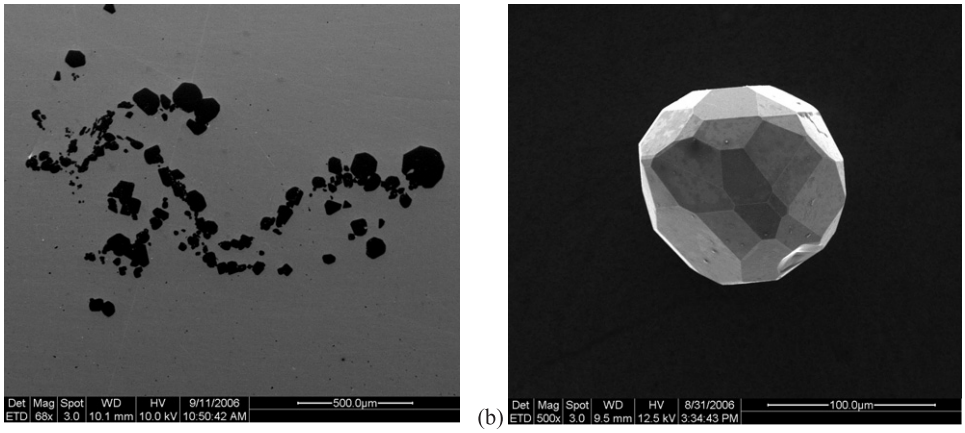


**Figure 1.** SEM images from (a) $CoP_3$ single crystals embedded in the Sn flux, and (b) example of a single crystal after etching away the Sn flux as described in the text.

**Table 1.** The cell parameter $a$ of $CoP_3$ obtained in this study, compared with that of previous workers.

| | Cell parameter, $a$ (pm) |
|---|---|
| This work | 770.8 |
| Watcharapasorn *et al* (1999) | 770.73 |
| Jeitschko *et al* (2000) | 770.5 |

refined using the general structure analysis system (GSAS) (Larson and Von Dreele 2004) with the interface EXPGUI (Toby 2001). The XRD analysis showed that the synthesized crystals, shown in figure 1(b), consisted of a single phase, with a diffraction pattern corresponding to the cubic $CoP_3$ skutterudite. The cell parameter obtained, $a$, together with that reported by previous workers, is shown in table 1.

XPS and XAES were performed on $CoP_3$ crystals embedded in the Sn matrix using a VG Scientific ESCALAB Mk II fitted with a Thermo Electron Corporation Alpha 110 hemispherical analyser and Mg K$\alpha$ radiation ($h\nu = 1253.6$ eV). Survey and high-resolution spectra were acquired at pass energies of 100 and 20 eV respectively. Several areas (crystals) were analysed to ensure reproducibility of results. The use of the continuous Bremsstrahlung radiation generated by the 12 keV electrons entering the target enabled excitation of P 1s electrons with accompanying emission of P KLL Auger electrons (Castle and West 1979, 1980). The surface of the sample was analysed after Ar ion etching (4 keV) for 6 min until the C 1s and O 1s signals were minimized. By monitoring the Co and P 2p as well as the C and O 1s peak intensity during etching we were confident that etching did not affect the sample stoichiometry, but it only diminished the surface contamination. Data processing was performed using the CasaXPS software (www.casaxps.com).

### *2.2. Auger parameter and charge transfer calculations*

A common practice to reduce energy referencing effects utilizes binding energy shifts between two different chemical environments. This shift ($\Delta E$) can be expressed as

$$\Delta E_{(i)} = \Delta U - \Delta R. \tag{1}$$

The first term expresses initial-state contributions arising from the dependence of the potential to the changes in valence charge as well as from the Coulomb interaction between the photoelectron and the surrounding charged atoms. $\Delta R$ is the final-state contribution expressed as the relaxation energy change arising from the response of the atomic and extra-atomic environment to the screening of the core hole. The higher the electronic polarizability of the surrounding electron cloud is, the larger the relaxation energy becomes. However, the best practice to eliminate energy referencing involves measurement of the energy separation between two different spectral features on the same spectrum and subsequent comparison of this separation between different chemical environments. This was the initial concept of the Auger parameter ($\alpha$) as introduced by Wagner (1975) and modified by Gaarenstroom and Winograd (1977), who showed that energy referencing problems are completely removed by using the sum of the ionization energy ($I$) and the kinetic energy of the Auger electron ($K$) involving the same primary excitation. They defined therefore the modified Auger parameter $\alpha'$ as follows:

$$\alpha' = I + K. \tag{2}$$

The difference in the Auger parameter between two different states 1 and 2 is given by

$$\Delta\alpha' = \alpha'_1 - \alpha'_2 = \Delta I + \Delta K. \tag{3}$$

The above definition of $\alpha'$ separates final-state from initial-state effects, and it is known as the final-state Auger parameter. By assuming all core level shifts between two different environments to be the same, it can be shown that the changes in the final-state Auger parameter $\Delta\alpha'$ are equal to twice the change in relaxation energy ($\Delta R$):

$$\Delta\alpha' = 2\Delta R = 2(\Delta R^{\mathrm{val}} + \Delta R^{\mathrm{ea}}) \tag{4}$$

where $\Delta R^{\mathrm{val}}$ is the change in $\Delta R$ due to differences in the number of final-state valence electrons and $\Delta R^{\mathrm{ea}}$ is the contribution due to changes in extra-atomic relaxation (Moretti 1998). In general, large $\alpha'$ values are observed in metals and semiconductors due to superior electron screening, while smaller ones are observed for insulators. Equation (4) is not reliable for transition metals (Kleiman and Landers 1998), where d–s interband charge transfer has to be taken into account.

Thomas and Weighman (1986) have developed a model relating Auger parameter changes to initial-state atomic charge transfer, electron screening and polarization of the surroundings:

$$\Delta\alpha' = \Delta[q(\mathrm{d}k/\mathrm{d}N) + (k - 2\,\mathrm{d}k/\mathrm{d}N)(\mathrm{d}q/\mathrm{d}N) + (\mathrm{d}U/\mathrm{d}N)] \tag{5}$$

where $k$ is the change in core potential when a valence atom is removed, $q$ is the valence charge, $N$ is the occupancy of core orbitals and $U$ represents the contribution from the chemical environment. The above model assumes that $k$ and $q$ depend linearly on $N$. Further development of the model has taken into account the dependence of $k$ on the valence charge (Cole *et al* 1994, Cole and Weightman 1994).

## 3. Results and discussion

### *3.1. P and Co 2p core level and Co–P bond ionicity*

Figure 2 shows the Mg K$\alpha$ excited P 2p and 2s peaks together with their plasmon peaks. The Sn 4s peak is also shown, since the $CoP_3$ crystals were embedded in the Sn matrix (figure 1(a)) and the irradiated area is large enough (a few $mm^2$) to pick up signal from the Sn matrix surrounding the $CoP_3$ crystals. Small-area XPS was not performed because the use of a monochromator would not allow for the Bremsstrahlung induced excitation of the P KLL. The peak–plasmon separation was found to be 22.2±0.5 and 22.5±0.5 eV for the P 2p and P 2s peaks respectively.

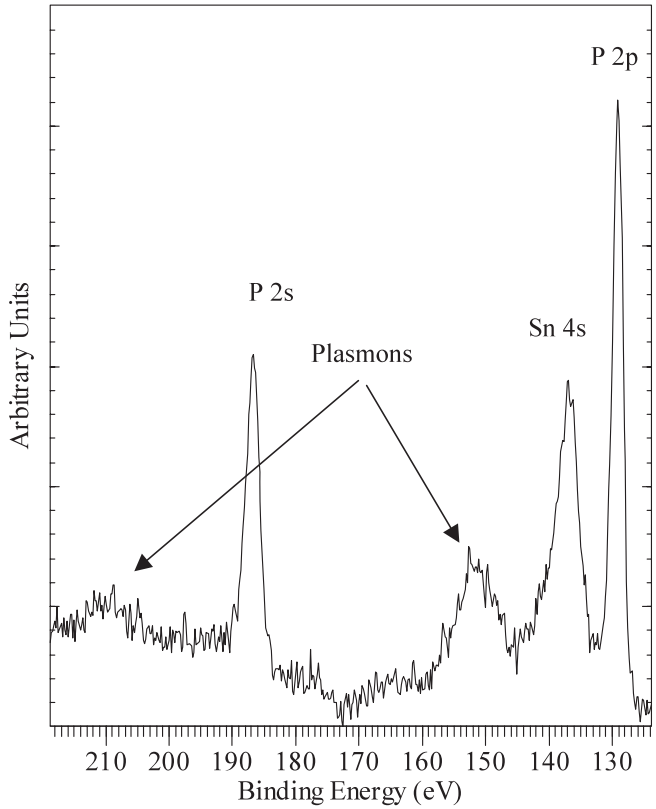


**Figure 2.** P 2p, P 2s high-resolution XPS spectra of $CoP_3$ and the associated plasmons. The Sn 4s of the Sn matrix is also shown.

These values are in good agreement with the plasmon energy of 21.7 eV obtained by electron energy-loss spectroscopy (Prytz *et al* 2006).

The Co and P 2p binding energy values are listed in table 2 together with the literature values (Wagner *et al*—NISTdatabase). We observe a shift towards lower binding energies for both Co and P 2p peaks, compared to the binding energies in the elemental solids. The shift for P 2p was found to be −0.8 eV compared with pure P whilst the shift for Co 2p was smaller (−0.4 eV). In comparison, previous studies of CoP (Grosvenor *et al* 2005) and $Co_2P$ (Nemoshalenko *et al* 1983) report virtually zero or small (−0.2 eV) shift in the Co 2p binding energy of CoP and $Co_2P$ respectively, while the binding energy of P 2p was lowered by 0.5 eV in CoP and 0.6 eV in $Co_2P$. For $CoP_3$, Grosvenor *et al* monitored a positive shift (+0.4 eV) for Co 2p in $CoP_3$ compared to pure Co, accompanied with a significant reduction (−0.7 eV) of the P 2p considering white P in elemental form (Grosvenor *et al* 2006). We attribute the opposite shifts of Co 2p in $CoP_3$ between the present study and that of Grosvenor *et al* (2005) to energy referencing issues. In measuring the chemical shift we used the literature value for pure Co 2p and this could well be the reason for the discrepancy. Absolute energy values depend on the sample/spectrometer work function, and this can be important when, for example, different spectrometers are used. For this reason we focus our analysis on the use of the Auger parameter which, as explained in section 2.2, is completely free of energy referencing inconsistencies. For $CoSb_3$ no shift in Co 2p and a very small one (−0.1 eV) for Sb were observed. Grosvenor *et al*

**Table 2.** Peak positions of Co and P 2p obtained from $CoP_3$ and literature values. Photoelectron peaks are given in binding energy.

| Compound | Co $2p_{3/2}$ (eV) | P 2p (eV) | $\Delta E_b$[a] (eV) |
|---|---|---|---|
| $CoP_3$ | 777.9 | 129.2 | 648.7 |
| Pure Co (lit) | 778.3 | | |
| Pure P white (lit) | | 130.0 | |
| CoP (lit) | 778.4 | 129.5 | 648.9 |
| $Co_2P$ (lit) | 778.2 | 129.4 | 648.8 |
| Phosphides[b] | | 129.1 | |
| Co oxides, sulfides[c] | 780.5 | | |
| Co and P ionic[d] | | | 651.4 |
| Co and P covalent[e] | | | 648.3 |

[a] $\Delta E_b$: difference in Co 2p and P 2p binding energy.
[b] Average of P 2p literature values of various phosphides (http://srdata.nist.gov/xps/).
[c] Average of Co 2p literature values of various oxides and sulfides (http://srdata.nist.gov/xps/).
[d] Subtraction of P 2p values in b from Co 2p values in c.
[e] Subtraction of P 2p value of pure P from the Co 2p value of pure Co.

interpreted that as evidence for a greater covalent character of the antimonides compared to phosphides. In their study the ionic character of the Co–P bond in $CoP_3$ was further supported by monitoring the intensity of the Co 2p energy loss peak (Grosvenor *et al* 2006). The observed reduction of the intensity of the loss feature in $CoP_3$ compared to pure Co was interpreted as a reduction of the Co valence electrons. Their interpretation differs from that of Hillebrecht *et al* for the Ni 2p shake up satellite (Hillebrecht *et al* 1983), who attributed its presence to a high density of unoccupied states just above $E_F$ and the sharp decrease in satellite intensity to the filling of the Ni 3d band. The use of unmonochromated Mg K$\alpha$ x-ray radiation did not allow us to measure accurately the intensity ratio between the satellite and the Co 2p main peak, due to the overlap of the x-ray satellite (Mg K$\alpha_4$) with the shake up satellite. The x-ray satellite of Co $2p_{1/2}$ appears at ∼5–6 eV higher than the Co $2p_{3/2}$ peak. This is approximately the energy regime of the occurrence of the Co $2p_{3/2}$ shake up (or plasmon) satellite. An attempt to subtract the x-ray satellite gave an $I_{sat}/I_{Co\ 2p}$ value of 0.06, which is close to the 0.1 reported for $CoP_3$ by Grosvenor *et al* (2006).

The difference in electronegativity between Co and P is not large: cobalt has an electronegativity of 1.88 in Pauling units, while for phosphorus the value is 2.19 (Atkins 1991). These values would suggest charge transfer from Co towards P, which should manifest itself in the XPS spectrum as a shift of the Co 2p peak to higher binding energies and that of P 2p to lower binding energies. Thus, the Co 2p–P 2p binding energy separation in ionic compounds should be larger than in covalent compounds. As shown in figure 3 and table 2, the Co 2p–P 2p energy separation of the $CoP_3$ compounds is higher than that obtained considering pure Co and P (covalent bonding), and comparable to previously reported values of CoP and $Co_2P$. The energy separation for $CoP_3$ and other Co–P compounds in figure 3 is significantly smaller than what is observed in very ionic environments such as Co in for example oxides and sulfides and P in other phosphides. Therefore the Co–P bonding should not be considered as strongly ionic, but rather as covalent with a partial ionic character. Previous studies on CrP, MnP, FeP and CoP showed a decreased ionicity of the metal–phosphorus bond on progressing from CrP to CoP. In addition, experimental valence band spectra coupled with theoretical studies indicated that the metal $t_{2g}$ states (one component of the 3d crystal-field splitting) increases through the series CrP to CoP (Grosvenor *et al* 2005). It was suggested that these states are due to metal–metal bonding and their increase was in agreement with the shortening of the average

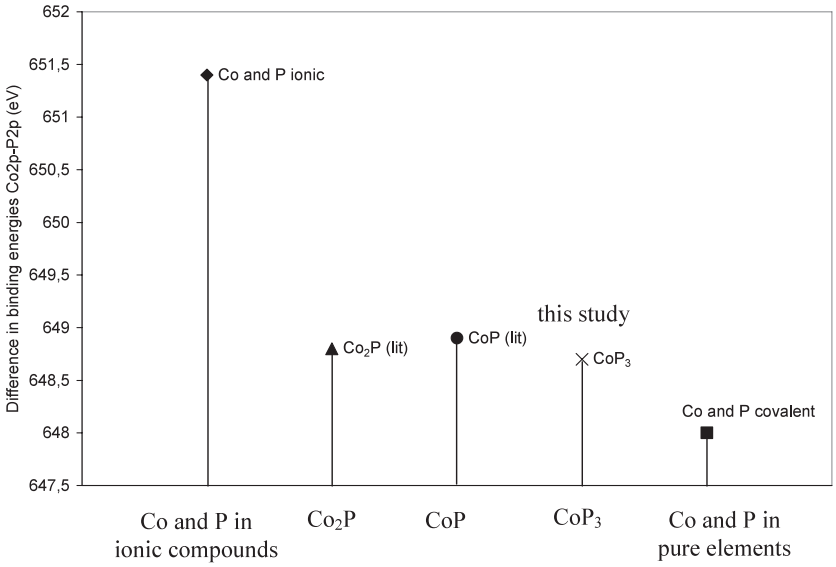


**Figure 3.** Comparison of Co 2p–P 2p energy separation between Co phosphides (from the literature and the current study) and the boundary conditions of Co and P in both ionic and covalent (pure elemental) environments.

**Table 3.** Co and P Auger parameter values obtained for $CoP_3$ and literature values for pure Co and P in several allotropes and compounds. Photoelectron and Auger peaks are given in binding and kinetic energy respectively.

| | Co $2p_{3/2}$ (eV) | P 2p (eV) | Co LMM (eV) | P KLL (eV) | Co 2p-LMM AP ($\alpha'$) (eV) | P 2p-KLL AP ($\alpha'$) (eV) |
|---|---|---|---|---|---|---|
| $CoP_3$ | 777.9 | 129.2 | 597.6 | 1858.7 | 1375.5 | 1987.9 |
| Pure Co (lit) | 778.3 | | 598 | | 1376.3 | |
| Pure P white (lit) | | 130.0 | | 1857.2 | | 1987.2 |
| $ZnP_2$ (lit) | | 129.6 | | 1857.3 | | 1986.9 |
| $Zn_3P_2$ (lit) | | 138.65 | | 1858.2 | | 1986.85 |
| $P_4S_{10}$ (lit) | | 133.05 | | 1853.45 | | 1986.5 |
| GaP (lit) | | 129.2 | | 1857.5 | | 1986.7 |
| InP | | 128.65 | | 1858.65 | | 1987.3 |

metal–metal bond lengths. Similarly, the population of the P 3p states involved in the P–P and TM–P bonding decreases in agreement with the increase in the length of the P–P bond. The valence band spectrum in our study was dominated by the Sn 3d band and therefore was of no analytical use. However, our results regarding Co–P ionicity are in general agreement with the trend shown in the monophosphides study (Grosvenor *et al* 2005).

### *3.2. The Auger parameter and charge transfer*

Table 3 shows Co 2p-LMM and P 2p-KLL $\alpha'$ values for $CoP_3$ from this study as well as P $\alpha'$ values from the literature for P-containing compounds (XPS database). The Co $LM_{23}M_{23}$ peaks in figure 4 were used together with the Co $2p_{3/2}$ (not shown) for the measurement of $\alpha'$ for Co whilst the P 2p and P KLL shown in figures 2 and 5 respectively were used for the P Auger parameter (AP) values. The use of $\alpha'$ allows us to probe the response of the core

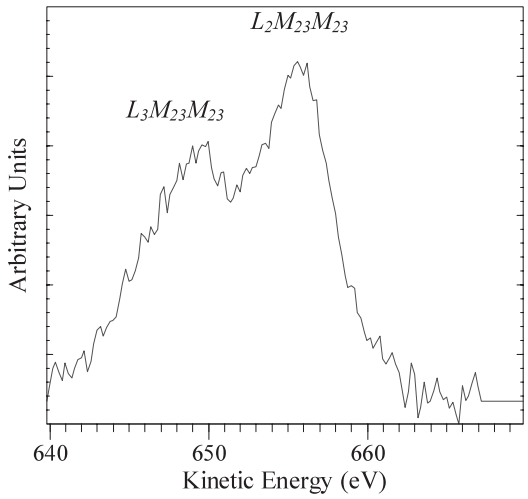


**Figure 4.** High-resolution Co LMM after subtraction of a Shirley-type background.

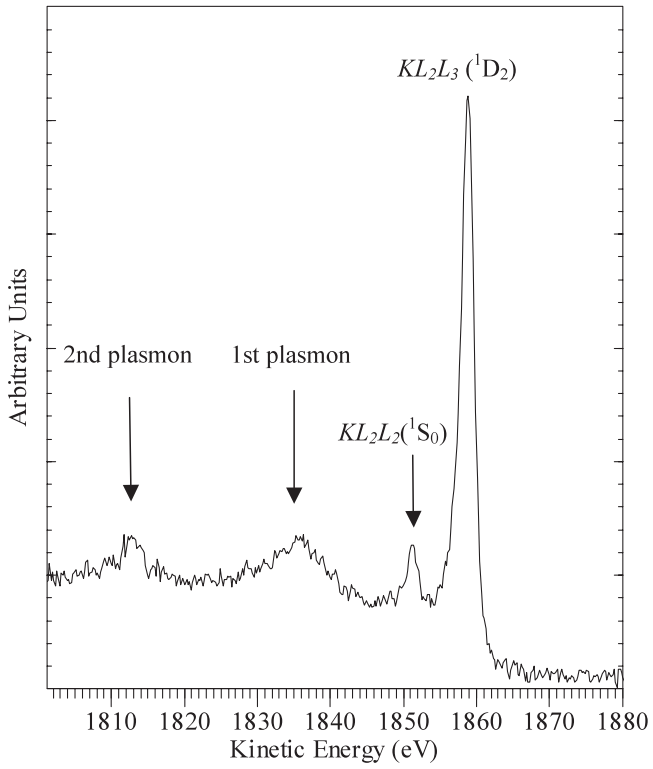


**Figure 5.** High-resolution Bremsstrahlung induced P KLL of $CoP_3$. The energy of the P KLL plasmon as determined by the separation between the main peak and the first plasmon peak, as well as between the first and second plasmon peak, is $22.8 \pm 0.5$ eV.

potential to changes in the atomic environment when localized core levels and core–core–core (CCC) Auger transitions are used. For this reason we used the Co $L_{23}M_{23}M_{23}$ peak (CCC transition) instead of the most intense $L_2M_{23}M_{45}$ which corresponds to a core–core–valence

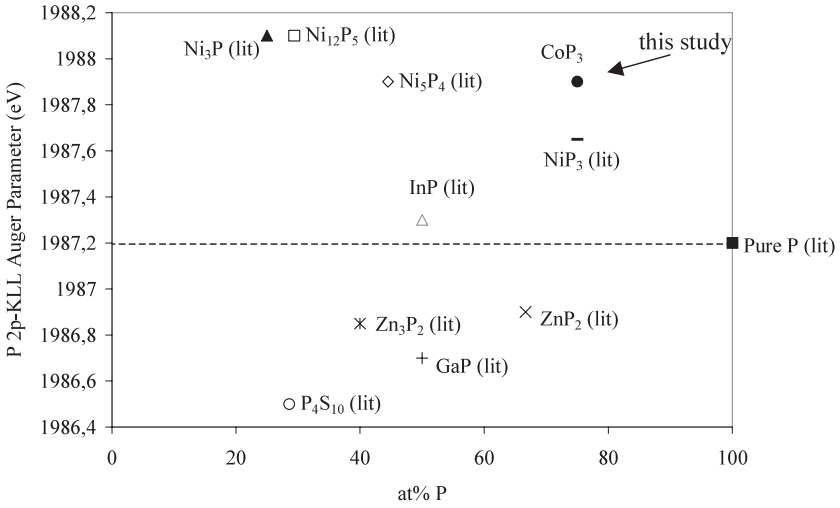


**Figure 6.** Comparison of P 2p KLL Auger parameter values between $CoP_3$ in this study and the literature values for pure P, metal phosphides and a phosphorus pentasulfide.

(CCV) transition. As shown in both figure 6 and table 3, $\alpha'$ for P in $CoP_3$ (and in the literature Ni–P compounds) is larger than the literature value for pure P. On the other hand the $\alpha'$ value for Co in $CoP_3$ is reduced compared to that for pure metal. Furthermore, as shown in figure 6, the value of $\alpha'$ for P in InP, $ZnP_2$, $Zn_3P_2$, GaP and $P_4S_{10}$ are close to or smaller than the values for pure P.

In the case of metals, $\Delta\alpha'$ in (5) can be interpreted as charge transfer ($\Delta q$) since the second and third terms in equation (5) become zero due to the assumption of perfect screening ($\mathrm{d}q/\mathrm{d}N = 1$) and highly polarizable surroundings ($\Delta U = 0$). In this context the increase of the P AP would correspond to a negative $\Delta q$, thus indicating electron donation from Co to P ($\mathrm{d}k/\mathrm{d}N$ in equation (5) is a negative quantity). However, in covalent semiconductors such as Si and P the radial maximum of $sp^3$ hybrid orbitals is greater than the inter-nuclei distance of adjacent sites and thus it is expected that these compounds are characterized by delocalized screening. In this context the last two terms in equation (5) are important.

The higher $\alpha'$ of P in $CoP_3$ compared to pure P shows an increased core hole screening efficiency and therefore demonstrates a 'metallic' character of the $CoP_3$ in the same context as Ni–P compounds in previous studies (Franke *et al* 1991, Franke 1987). In contrast, $\Delta\alpha'$ of Co shows the opposite behaviour as we move from pure Co to $CoP_3$. Assuming a metallic character of the $CoP_3$ compound, both Co and P AP changes can be interpreted in terms of electron transfer. Using equation (5) for the metal case we calculate the charge transfer for P for s- and p-type to be $-0.34$ and $-0.24$ $e^-$/atom respectively (see table 4) with the negative sign denoting electron gain. In the periodic table, phosphorus ($3s^23p^3$) is followed by sulfur ($3s^23p^4$), and according to the equivalent cores approximation it is more likely for a core hole in the photoionized P atom to be screened by a p valence electron than by an s electron. This is particularly important in the context of p–d coupling and/or s–p–d hybridization. In both cases the contribution of P 3p and Co 3d charge is a central issue. EELS suggested (Prytz *et al* 2007) that Co donates 0.77 $e^-$/Co atom. From stoichiometric considerations one Co atom corresponds to three P atoms in $CoP_3$; therefore, P gains $0.77/3 = 0.26$ $e^-$/atom. We see that the above value lies closer to p-type charge transfer for P.

We now consider the Co contribution to charge transfer. Assuming that the differences in d screening following ionization are equal to differences in d charge (Thomas and Weighman

**Table 4.** $\Delta R^{ea}$ values, charge transfer values and potential parameters used for the charge transfer calculations of P and Co in $CoP_3$. A positive sign in the charge transfer values denotes electron donation and a negative sign electron gain.

| Element | $\Delta R^{ea}$ [a] (eV) | $dk/dN_P$ [a] (eV) | $dk/dN_{Co}$ [b] (eV) | $dk'/dN_{Co}$ [b] (eV) | s-charge transfer ($e^-$/atom) | p-charge transfer ($e^-$/atom) | d-charge transfer ($e^-$/atom) |
|---|---|---|---|---|---|---|---|
| P s charge | | −2.04 | | | −0.34 | | |
| P p charge | | −2.09 | | | | −0.24 | |
| Co s charge | | | −2.27 | −4.09 | 0.08 | | |
| Co d charge | | | −4.57 | −4.60 | | | +0.27 to +0.93 |
| P | +0.462 | | | | | | |
| Co | −0.4 | | | | | | |

[a] Values taken from Jackson *et al* (1995).
[b] Values taken from Gregory *et al* (1993).

1986), equation (5) can be written as

$$\Delta\alpha = \Delta q_d(\,dk_d/\,dN - \,dk_s/\,dN) + \Delta q_s(\,dk_s/\,dN). \tag{6}$$

The terms $dk_s/dN$ and $dk_d/dN$ are the potential parameters (see table 4) for the s shell and d shell respectively (Gregory *et al* 1993), whilst $\Delta q_d$ and $\Delta q_s$ are the charge transfer contribution of the Co d band and s band respectively. Assuming overall charge neutrality, the Co s valence band contribution is given by

$$x\Delta q_s^{(Co)} = -(1-x)\Delta q^{(P)} \tag{7}$$

where $x$ is the P molar fraction (0.75) and $\Delta q^{(P)}$ is the P charge transfer. Considering only p-type P charge we calculate the s- and d-type Co charge transfer. Using equations (6) and (7) and the two sets of potential parameters in table 4, we calculate $+0.27$ $e^-$/atom $\leqslant \Delta q_d^{Co} \leqslant$ $+0.93$ $e^-$/atom (table 4). The higher value in the above range corresponds to potential parameters for free atoms and the lower for potential parameters normalized in order to take into account the compression of the valence band in the solid (Thomas and Weighman 1986, Gregory *et al* 1993). We recall that the electron transfer away from Co deduced from EELS investigations (Prytz *et al* 2007) was 0.77 $e^-$/atom. This lies within the 0.27–0.93 $e^-$/atom range as estimated with XPS in this study. The accuracy of the estimated charge transfer would depend, to a certain extent, upon the choice of the potential parameters incorporated in the calculations. For the P contribution to charge transfer we used potential parameter values (Jackson *et al* 1995) which take into account the nonlinear dependence of $k$ and $q$ on N. For the Co contribution the only literature data we found (Gregory *et al* 1993) referred to potential parameters which were calculated assuming a linear dependence of $k$ and $q$ on $N$.

In the above analysis P was treated as having 'metallic' behaviour in $CoP_3$ due to the increased screening compared to pure P and other P-containing compounds with known semiconducting or insulating behaviour (see figure 6 and table 5). However, it is possible that, due to its semiconducting nature, $\Delta\alpha'$ for P could reflect differences in screening efficiency as represented in Weightman's models by the dielectric constant (Weightman 1998) rather than charge transfer. Although electrical and optical measurements on $CoP_3$ have suggested the presence of a small band gap, the semiconducting nature of the compound is in doubt due to disagreements amongst calculations (Grosvenor *et al* (2006) and references 10, 13, 15 and 16 therein). Therefore, the metallic character of the compound is not an unreasonable assumption and the phosphorus AP dependence on initial-state charge transfer gains ground.

The use of the Bremsstrahlung induced P KLL peak has an additional advantage. The matrix element of an Auger process usually involves the wavefunction of a core orbital and

**Table 5.** Band gap values for various TM phosphides shown in figure 5 and difference in s and d orbital radius between Co and various TMs. Values refer to free atoms. A positive difference means that the Co radii are larger.

| Compound elements | Compound | Difference in s orbital radius[a] between TMs (%) | Difference in d orbital radius[a] between TMs (%) | Band gap (eV) |
|---|---|---|---|---|
| Co–Ni | | +3.4 | +5.9 | |
| Co–In | | +6.9 | +27.1 | |
| Co–Zn | | +9.9 | +17.8 | |
| Co–Ga | | +24.7 | +25.6 | |
| | InP | | | 1.42[b] |
| | $Zn_3P_2$ | | | 1.5[c] |
| | $\alpha$-$ZnP_2$ | | | 2.05[d] |
| | CaP | | | 2.32[a] |

[a] Radii values taken from www.webelements.com.
[b] Kittel (1986).
[c] Suda and Kakishita (1996).
[d] Käräjämäki *et al* (1980).

the Auger transition will only sample the local electronic structure (Matthew and Komninos 1975). Thus, the localized character of the final states of the Auger transition contrasts the delocalized nature of screening in semiconductors such as P (see also section 3.3); therefore it is difficult to distinguish contributions of the local and non-local density of states (DOS) in Auger profiles of semiconductors involving the valence band (Weightman 1998). By acquiring the Bremsstrahlung induced P KLL in the present study we probe only core levels and we overcome the above problem probing thus only the P DOS.

### *3.3. The Auger parameter and changes in polarizability/screening efficiency*

It has been shown that the shift of P 1s ($\Delta P_{1s}$) is different from that of P 2p ($\Delta P_{2p}$), and more precisely $m = \Delta P_{1s}/\Delta P_{2p} \approx 1.14$ (Moretti 1998 and references 88, 89, 90 therein). Therefore, equation (4) changes to

$$\Delta\alpha = 2\Delta R + (m-1)\Delta E_{2p} = 2\Delta R + 0.14\Delta E_{2p}. \tag{8}$$

$\Delta E_{2p}$ between pure P and P in $CoP_3$ is a negative quantity (see table 2). Equation (8) shows that, without correcting for unequal P 1s and P 2p shifts, the increase in relaxation energy accompanying photoelectron and Auger electron emission (and/or P core hole electron screening) in $CoP_3$ as compared to pure P is underestimated. Using equation (8) and tables 2 and 3 we measure the relaxation energy ($\Delta R$) associated with the emission of 2p photoelectrons and the associated KLL and LMM Auger electrons in the P and Co atoms of $CoP_3$ (see table 4). $\Delta R$ between P in $CoP_3$ and in pure P is +0.46 eV. Accordingly the $\Delta R$ value for Co is −0.4 eV. The negative sign indicates a reduction in the extra-atomic relaxation (and/or screening) energy in the case of Co in $CoP_3$.

Although to a good approximation $\Delta\alpha$ is only related to final-state effects in the form of the relaxation energy ($\Delta R$) transferred from the surroundings to the photoionized atom, the electronic polarizability of the surroundings also depends on the nature of chemical bonding. Therefore apart from initial-state effects (Madelung potential, charge transfer), the final-state effects also depend on the ground-state properties of the system (Moretti 1990 and references 1–4 therein). The position of $CoP_3$ in figure 6 can be interpreted in terms of the polarizability of the surrounding electrons. As we progress from Co to Ni, Zn, Ga, In, the valence band of

the metal becomes more localized and therefore less polarizable (see table 5). The P atoms in $NiP_3$, InP, $Zn_3P_2$, $ZnP_2$, and GaP are surrounded by less polarizable electrons compared to P atoms in $CoP_3$. As mentioned in section 1, P in $CoP_3$ has two Co and two P nearest neighbours. The reduced polarizability of the valence electrons in the Ni–P compounds compared to $CoP_3$ is counterbalanced by the increased number of the average P–Ni ligands in $Ni_5P_4$, $Ni_{12}P_5$ and $Ni_3P$. In these compounds the Ni-rich environment of the P atoms provides polarizable electrons which screen the P core hole more effectively than the P-rich environment of P atoms in $NiP_3$.

An alternative explanation of the relative positions of the compounds in figure 6 can be given by considering the band gaps of the semiconductors (see table 5). The increase in band gap would lead to a reduction in screening efficiency (as shown by the lower $\alpha'$ value) since the conduction electrons would 'strangle' more to screen a core hole. However, such an explanation should have as a prerequisite that the relative position of the Fermi level does not vary significantly from compound to compound and that we assume more or less 'intrinsic' semiconductors.

## 4. Conclusions

The Co–P 2p binding energy difference indicates that the Co–P bonding in $CoP_3$ is covalent with partial ionic character. We used the Bremsstrahlung radiation to acquire the P KLL Auger peak and to measure the P 2p KLL Auger parameter. The reduced P 2p KLL Auger parameter of pure P compared to $CoP_3$ showed that the P core holes are screened better in the compound than in the pure element, while the Co 2p LMM Auger parameter showed that electron screening of the Co core holes is stronger in the elemental environment. Considering a metallic environment for the P atoms in $CoP_3$ compared to pure P, the charger transfer between Co and P atoms was estimated using Auger parameter data and the Thomas and Weightman model. It is suggested that upon bonding to form the $CoP_3$ compound, Co donates 0.27–0.93 $e^-$/atom and P gains 0.24 $e^-$/atom. These values correspond well with Co losing 0.77 $e^-$/atom as deduced from previous EELS studies and thus P gaining $0.77/3 = 0.26$ electrons/atom (Co:P = 1:3). Additional explanations of the increased P Auger parameter in $CoP_3$ compared to other P-containing compounds include a reduced band gap and an increased polarizability of the P atomic environment in this compound.

## Acknowledgment

Financial support from FUNMAT@UiO to one of us (ØP) is gratefully acknowledged.

## References

Anno H, Matsubara K, Caillat T and Fleurial J-P 2000 *Phys. Rev.* B **72** 10737
Atkins PW 1991 *Quanta—A Handbook of Concepts* 2nd edn (Oxford: Oxford University Press)
CasaXPS http://www.casaxps.com
Castle J E and West R H 1979 *J. Electron Spectrosc. Relat. Phenom.* **16** 195
Castle J E and West R H 1980 *J. Electron Spectrosc. Relat. Phenom.* **18** 355
Cole R J, Gregory D A C and Weightman P 1994 *Phys. Rev.* B **49** 5657
Cole R J and Weightman P 1994 *J. Phys.: Condens. Matter* **6** 5783
Dudkin L D 1958 *Sov. Phys. Tech.—Phys.* **3** 216
Fornari M and Singh D J 1999 *Phys. Rev.* B **59** 9722
Franke R 1987 *Spectrochim. Acta* A **53** 933
Franke R, Chasse Th, Streubel P and Meisel A 1991 *J. Electron Spectrosc. Relat. Phenom.* **56** 381

Gaarenstroom S W and Winograd N J 1977 *J. Chem. Phys.* **67** 500
Gregory D A C, Laine A D, Fowles P S, Takahashi A and Weightman P 1993 *J. Phys.: Condens. Matter* **5** 3843
Grosvenor A P, Cavell R G and Mar A 2006 *Phys. Rev.* B **74** 125102
Grosvenor A P, Wik S D, Cavell R G and Mar A 2005 *Inorg. Chem.* **44** 8988
Hillebrecht F U, Fuggle J C, Bennett P, Zolnierek Z and Freiburg C 1983 *Phys. Rev.* B **27** 2179
Jackson M D, Cole R J, Brooks N J and Weightman P 1995 *J. Electron Spectrosc. Relat. Phenom.* **72** 261
Jeitschko W, Foecker A J, Paschke D, Dewalsky M V, Evers C B H, Künnen B, Lang A, Kotzyba G, Rodenwald U C and Möller M H 2000 *Z. Anorg. Allg. Chem.* **626** 1112
Käräjämäki E, Laiho R and Levola T 1980 *J. Phys. C: Solid State Phys.* **13** 3977
Keast V J, Scott A J, Brydson R, Williams D B and Burley J 2001 *J. Microsc.* **203** 135
Kittel C 1986 *Introduction to Solid State Physics* 6th edn (New York: Wiley)
Kjekshus A and Pedersen G 1961 *Acta Crystallogr.* **14** 1065
Kjekshus A and Rakke T 1974 *Acta Chem. Scand.* A **28** 99
Kleiman G G and Landers R 1998 *J. Electron Spectrosc. Relat. Phenom.* **88** 435
Koga K, Akai K, Oshiro K and Matsuura M 2005 *Phys. Rev.* B **71** 155119
Larson A L and Von Dreele R B 2004 General structure analysis system (GSAS) *Los Alamos National Laboratory Report* LAUR 86-748, Los Alamos National Laboratory, Los Alamos
Lefebvre-Devos I, Lassalle M, Wallart X, Olivier-Fourcade J, Monconduit L and Jumas J C 2001 *Phys. Rev.* B **63** 125110
Llunell M, Alemany P, Alvarez S, Zhukov V P and Vernes A 1996 *Phys. Rev.* B **53** 10605
Løvvik O M and Prytz Ø 2004 *Phys. Rev.* B **70** 195119
Matthew J A D and Komninos Y 1975 *Surf. Sci.* **53** 716
Moretti G 1990 *J. Electron Spectrosc. Relat. Phenom.* **50** 289
Moretti G 1998 *J. Electron Spectrosc. Relat. Phenom.* **95** 95
Nemoshalenko V V, Didyk V V, Krivitskii V P and Senekevich AI 1983 *Zh. Neorg. Khim.* **28** 2182
Prytz Ø, Løvvik O M and Taftø J 2006 *Phys. Rev.* B **74** 245109
Prytz Ø, Taftø J, Ahn C C and Fultz B 2007 *Phys. Rev.* B **75** 125109
Singh D J and Pickett W E 1994 *Phys. Rev.* B **50** 11235
Suda T and Kakishita K 1996 *Appl. Phys. Lett.* **69** 2426
Thomas T D and Weightman P 1986 *Phys. Rev.* B **33** 5406
Toby B H 2001 *J. Appl. Crystallogr.* **34** 210
Uher C 2001 *Semicond. Semimet.* **69** 139
Wagner C D 1975 *Faraday Discuss. Chem. Soc.* **60** 291
Wagner C D, Naumkin A V, Kraut-Vass A, Allison J W, Powell C J and Rumble J R Jr 2003 (Compilation and evaluation) *NIST x-ray Photoelectron Spectroscopy Database-IST Standard Reference Database 20* version 3.4 *(Web Version)* http://srdata.nist.gov/xps/
Watcharapasorn A, DeMattei R C, Feigelson R S, Caillat T, Borshchevsky A, Snyder G J and Fleurial J P 1999 *J. Appl. Phys.* **86** 6213
www.webelements.com Webelements (accessed 20-11-2006)
Weightman P 1998 *J. Electron Spectrosc. Relat. Phenom.* **93** 165